

# Research on DTC System with Variable Flux for Switched Reluctance Motor

Xianchao Zhao, Aide. Xu, Wen Zhang

**Abstract**—When switched reluctance motor(SRM) is in the status of the traditional direct torque control(DTC) system, due to the high saturation nonlinearity of the electromagnetic relationships of switched reluctance motors, the torque ripple and the stator phase current are larger. In order to resolve the above problems, through the analysis and deduction for SRM flux model and the influence of characteristics of flux and speed on torque ripple, this paper presents a variable-flux control strategy with the three closed-loop structure based on the critical flux supersaturated speed. And a DTC system of SRM with variable flux and three closed-loop is built up in Matlab/simulink. Moreover, the DSP hardware experiment platform based on the TMS320F2812 is established to validate the performance of the improved algorithm. The simulation and experimental results show that the new scheme has an obvious effect on torque ripple reduction, and the three - phase stator current is obviously reduced, which greatly reduces the stator winding copper consumption during the operation of SRM. Moreover, the improved system has good system stability.

**Index Terms**—Critical flux supersaturated speed, direct torque control, switched reluctance motor, three closed-loop, variable flux

## I. INTRODUCTION

SWITCHED Reluctance Drive(SRD) is a new generation of stepless speed control system developed after DC speed and frequency control. As switched reluctance motor (SRM) has a series of advantages such as intrinsic simplicity, low cost, large starting torque, simple and reliable power circuit, which attract the general attention and in-depth research of the domestic and foreign scholars [1-2]. However, due to high nonlinearity of the electromagnetic relationship and double salient pole structure, the conventional control method can cause the high torque ripple of the motor, which limits its application in low torque pulsation.

For the problem of the high torque ripple of SRM speed control system, scholars at home and abroad have made a lot of research. Various control technologies have been presented for

torque ripple reduction of SRM, including feedback - linearization-based controller, adaptation technique [3-4], fuzzy control strategy [5-6] and synovial and iterative algorithms [7-8]. In [9-11], the torque ripple reduction is studied by the torque distribution function, but the control strategy is affected by the back electromotive force of the winding and the torque distribution function is difficult to choose. Due to good robustness, simple and direct control strategy, direct torque control is applied to the SRM speed control system. But the torque is usually out of control in the commutation zone[12]. For the phenomenon of torque runaway in the commutation zone, the space voltage vector optimization method is proposed to decrease the torque ripple in [13]. This method has achieved remarkable results, but it increases the complexity of the algorithm, the requirements for hardware circuit are higher. Nowadays, the neural network intelligent control algorithm has been widely used in torque ripple reduction. In [14-15], the neural network is used to coordinate the three parameters of the PID controller, so as to achieve the optimal control of the system. And the simulation results show the good dynamic performance. However, there are still a few shortcomings that the model is easy to fall into the local minimum and its convergence speed is slow in the training. Moreover, hardware implementation has many difficulties. Hence, this scheme has some limitations in the application. Although the direct torque control system of SRM has been studied in [16-18], the efficiency and stability of the system are not analyzed deeply or lacking specific experimental verification. Last but not least, the influence of speed on torque ripple is not taken into consideration.

Aiming at the above problems, this paper discusses the problems existing in the traditional DTC system for switched reluctance motor in detail. And through the theoretical analysis and deduction for the SRM flux model and characteristic of speed and flux, the variable-flux control strategy is put forward based on traditional direct torque control technology. Finally, through the simulations and experiments, the three closed-loop DTC system optimized by variable-flux control strategy is verified in aspects of efficiency, torque ripple reduction and stability.

## II. THE MATHEMATICAL MODEL OF SRM

### A. Voltage equation

According to the basic law of the circuit, the phase K's

This work was supported in part by the National Natural Science Youth Foundation of China (51407021) and the central university basic research business fee (3132015214).

Xianchao Zhao is with the Dalian Maritime University, Dalian, 116026 China (e-mail: 819112013@qq.com).

Aide Xu is with the Dalian Maritime University, Dalian, 116026 China (e-mail: aidexu@dlnu.edu.cn).

Wen Zhang is with the Dalian Maritime University Dalian, 116026 China (e-mail: zhangwen\_78@163.com).

voltage balance equation of the motor is:

$$U_k = R_k \cdot i_k + \frac{d\psi_k}{dt} \quad (1)$$

Where  $U_k$  — The winding voltage of the phase K;

$R_k$  — The winding resistance of the phase K;

$i_k$  — The winding current of the phase K;

$\psi_k$  — The winding voltage of the phase K.

### B. Flux model

In (1), the phase winding resistance drop  $i_k \cdot R_k$  is much smaller than  $d\psi_k / dt$ . Therefore, ignoring the resistance drop, the (1) can be simplified to [19]:

$$u_k = \frac{d\psi_k}{dt} = \frac{d\psi_k}{d\theta} \cdot \frac{d\theta}{dt} = \frac{d\psi_k}{d\theta} \cdot \omega_r \quad (2)$$

Where  $\theta$  — The relative position angle of the stator and rotor;

$\omega_r$  — The angular speed of the motor.

Further finishing:

$$d\psi_k = \frac{u_k}{\omega_r} d\theta \quad (3)$$

When the main switch device of this phase is turned on ( $\theta = \theta_{on}$ ), the initial value of the flux  $\psi = 0$ ,  $\theta_{on}$ : the relative position angle between stator and rotor at the moment of winding is powered, called the opening angle.

Integrating the (3) and substituting the initial conditions into it, the flux equation in the conduction phase is:

$$\psi_k = \int_{\theta_{on}}^{\theta} \frac{u_k}{\omega_r} d\theta = \frac{u_k}{\omega_r} (\theta - \theta_{on}) \quad (4)$$

When the main switch device of this phase is turned off ( $\theta = \theta_{off}$ ), the flux is maximized.  $\theta_{off}$ : the relative position angle between stator and rotor at the moment of winding is powered off, called the closing angle. The maximum of flux is:

$$\psi = \psi_{max} = \frac{u_k}{\omega_r} (\theta_{off} - \theta_{on}) = \frac{u_k}{\omega_r} \theta_c \quad (5)$$

$$\theta_c = \theta_{off} - \theta_{on}$$

Where  $\theta_c$  — The conduction angle of the stator phase winding.

After the main switching device is turned off, the initial value of the flux  $\psi$  is equivalent to  $\psi_{max}$  during the winding freewheeling, where:  $u_k = -U_s$ , integrating and substituting the initial conditions into (5), the flux equation in the shutdown phase is:

$$\psi_k = -\int_{\theta_{off}}^{\theta} \frac{U_s}{\omega_r} d\theta = \frac{U_s}{\omega_r} (2\theta_{off} - \theta_{on} - \theta) \quad (6)$$

From (6), when the  $\theta$  is equal to  $2\theta_{off} - \theta_{on}$ , the flux is attenuated to zero and remains at zero until the next cycle of the phase main switching device is turned on again.

According to the above analysis, we can draw the changing curve of the flux and the rotor position angle, as shown in Fig.1.

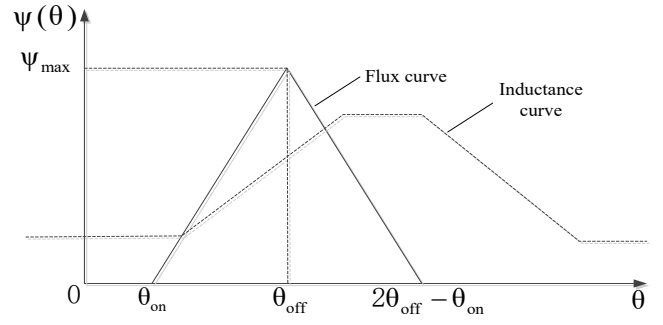


Fig. 1. The changing curve of flux and rotor position angle.

Thus, the relationship between the flux and the rotor position angle can be expressed as a function:

$$\psi_k = \begin{cases} \frac{U_s}{\omega_r} (\theta - \theta_{on}) & (\theta_{on} \leq \theta < \theta_{off}) \\ \frac{U_s}{\omega_r} (2\theta_{off} - \theta_{on} - \theta) & (\theta_{off} \leq \theta < 2\theta_{off} - \theta_{on}) \\ 0 & (\text{other position}) \end{cases} \quad (7)$$

## III. TRADITIONAL DTC SYSTEM FOR SRM

### A. The structure of traditional DTC system for SRM

The traditional DTC system for SRM usually includes the speed outer loop and the torque inner loop, as shown in Fig.2. The given torque is obtained after the speed adjustment. Then, a torque error signal obtained by making a difference with the feedback torque. Finally, combining the sector judgement signal and the error of given flux and feedback flux we can select the appropriate space voltage vector from the switch table, thereby realizing the control for SRM speed control system.

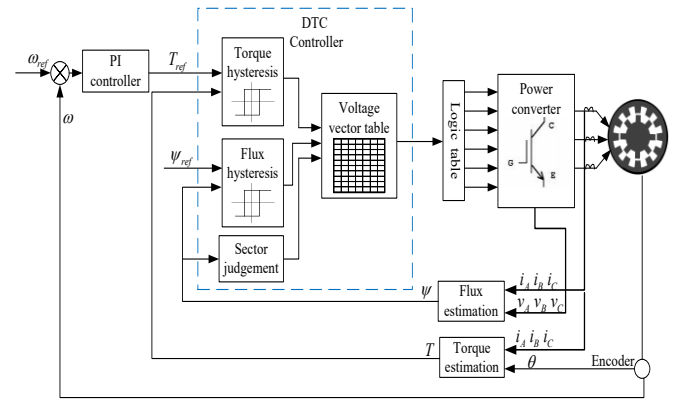


Fig. 2. The diagram of traditional DTC system.

### B. The principle of traditional DTC system for SRM

The ideology of the direct torque control technique is to keep the amplitude of the given flux constant, and regulate the torque within a hysteresis by adjusting the phase angle of the stator flux and the rotor flux, thereby suppressing its torque ripple and noise.

The literature [17] is carried out a detailed derivation for the (1). And getting the instantaneous torque equation of SRM:

$$T = i \frac{\partial \psi(i, \theta)}{\partial \theta} - \frac{dW_f}{d\theta} \quad (8)$$

Where  $T$  —The instantaneous torque of the motor;  
 $\psi(i, \theta)$  —The phase winding flux of the stator.

Due to high saturation characteristics of the SRM magnetic field,  $dW_f/d\theta$  is generally very small and negligible. Thus, the instantaneous torque equation is:

$$T \approx i \frac{\partial \psi(i, \theta)}{\partial \theta} \quad (9)$$

Since the phase winding of SRM is uni-polar driven, the current flowing through each phase winding is a forward current. It can be seen from (9) that the sign of the torque is determined by the sign of the partial term of the flux. So the output torque of the SR motor can be controlled by the advance or lag of stator flux relative to the rotor position, so that it can be controlled within a certain hysteresis. And according to  $\Delta\psi = u\Delta t$ , the control of the flux linkage can be converted to select the appropriate voltage vector to control the torque.

### C. The shortcomings of traditional DTC system for SRM

In the traditional SRM direct torque control system, in order to obtain a larger output torque, the given amplitude of the flux should be as large as possible (from 0.3 to 0.5), and the flux amplitude remains constant. However, according to the analysis of the characteristics for current and flux [20], when the motor is running at low speed, the characteristics of the flux and the current basically conform to the current-flux characteristic, the torque ripple is small, thereby the amplitude of flux can be constant.

Whereas, according to the (7), when the motor is running at high speed, the angular velocity increases with the increasing of speed, the amplitude of given flux required for the running of SRM becomes smaller than before. Thus, with the increasing of speed, the given flux should be gradually smaller. However, in the traditional SRM direct torque control system, the given flux is a constant value, which makes the given flux appears to be over-saturated and results in the error between the given flux and the feedback flux becoming larger and larger, then directly affect the selecting of space voltage vector, eventually leading to the higher torque ripple.

Moreover, with the increasing of speed, the actual given flux is gradually smaller. Therefore, we may as well set two different given flux amplitude  $\psi_{\max}$  and  $\psi_{\min}$  for further analysis. Then according to the Fig.1, we can obtain the magnetic flux curve under different given flux amplitude, as shown in the Fig.3. From the Fig.3, the changing rate of the flux linkage for the rotor position angle is different when given two different flux amplitude. Obviously, when the given flux is larger in a certain range, the changing rate of the flux linkage relative to the rotor position angle is larger. Therefore, according to (9), the changing rate of the flux linkage relative to the rotor position angle is larger, the partial derivative of the flux relative to angle increases, which results in the higher torque ripple.

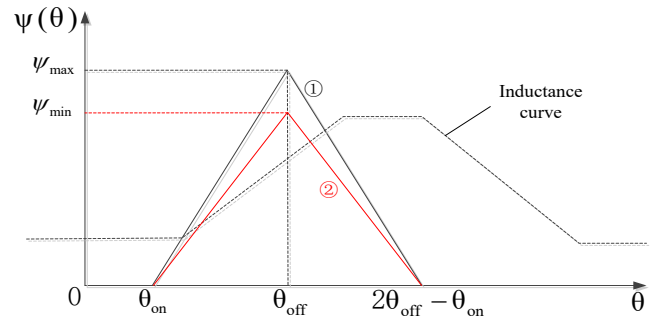


Fig. 3. The angle-flux curve in different given flux.

In addition, in order to obtain the larger output torque, the given flux usually is as large as possible, which makes the current larger. Thereby, it increases the stator winding copper consumption and reduces the operating efficiency of SRM.

Otherwise, in order to verify the correctness of the above analysis, the simulation results are shown in Fig.4 and Fig.5, when the given flux are 0.43Wb and 0.35Wb respectively.

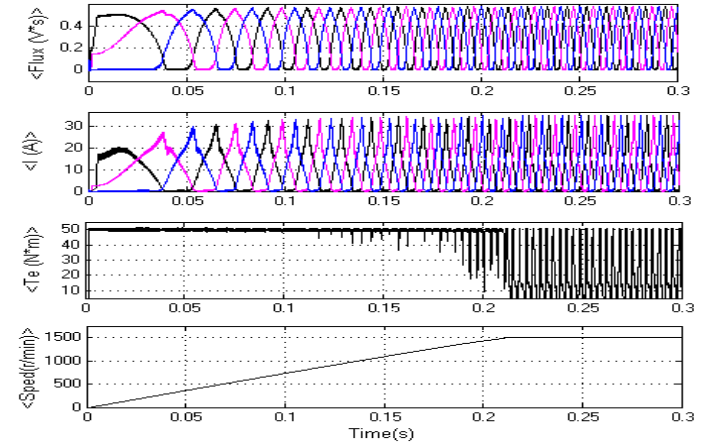


Fig. 4. The simulation result ( $\psi = 0.43\text{Wb}$ ).

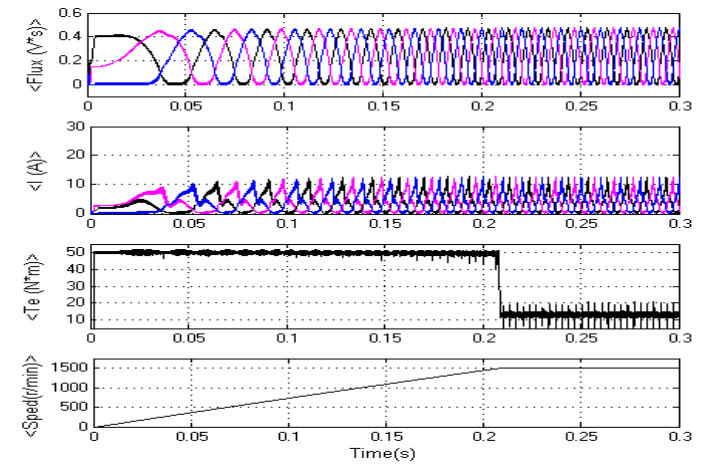


Fig. 5. The simulation result ( $\psi = 0.35\text{Wb}$ ).

According to the above analysis and simulation results, we can conclude that: due to the constant amplitude of given flux, the disadvantages of traditional DTC system for SRM include

high torque ripple and low running efficiency. Therefore, adopting the control ideology of variable flux into the traditional DTC system is significant for solving those problems. In addition, in order to take the system stability into consideration, the three closed-loop control structure is established.

#### IV. THREE CLOSED-LOOP DTC SYSTEM WITH VARIABLE FLUX

##### A. The structure of three closed-loop DTC system with variable flux

Aiming at the high torque ripple and low efficiency in traditional DTC system for SRM. The three closed-loop DTC system with variable flux is set up. The system is composed of torque loop and flux loop in parallel, which constitute the inner ring. Since the essence of the speed control system is to control the torque, and the core of the direct torque control is the flux[16]. Thus, it can be deduced that the variation of the flux is consistent with the required torque variation. According to the above analysis, the speed-flux loop can be modeled according to the speed-torque loop, and only need to make appropriate adjustments to the coefficients. In this way, the speed loop is used as the outer loop of the system, and its output is considered as the input of the variable-flux controller. The structure of system is shown in Fig.6.

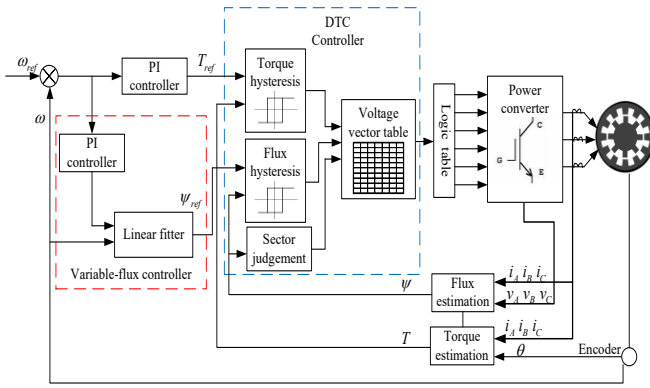


Fig. 6. The diagram of the three closed-loop DTC system with variable flux For SRM.

##### B. Critical flux supersaturated speed

###### 1) Definition of critical flux supersaturated speed

According to the analysis of the current-flux characteristics in [20], the actual flux and current characteristics basically conform to the ideal current-flux characteristic curve when the motor is running at low speed. And when the speed reaches a certain value, the actual current-flux characteristics no longer meet the ideal current-flux characteristics curve. The given flux becomes saturated excessively, thereby the torque ripple gradually increase with the increasing of speed. At this time, the actual flux and current characteristics no longer conform to the ideal current-flux characteristic curve. So we define the speed at the moment as the critical flux supersaturation speed.

###### 2) Selection criteria of critical flux supersaturated speed

Because of the different parameters of SRM, we can not accurately determine the corresponding speed when the

changing characteristics of current and flux do not meet the ideal current-flux characteristic curve. So, the definition standard of the critical flux supersaturated speed is: the critical flux supersaturated speed is defined when the torque ripple is once more than 10%. In addition, the different amplitude of given flux corresponds to the different critical flux supersaturated speed. However, in order to obtain a larger output torque, but not earlier to make the flux appears to be supersaturated, the initial amplitude of the given flux is 0.4Wb in this paper.

###### 3) Determination of critical flux supersaturated speed

Based on traditional DTC system, in order to obtain a wide load torque range, the given torque is set to 50N·m. Through a large number of simulation found that: when the speed of the motor reached at 750r/min, the torque ripple began to gradually increase beyond the allowable range of torque ripple, so the critical flux supersaturated speed is 750r/min under this operating conditions. The simulation results are shown in Fig.7.

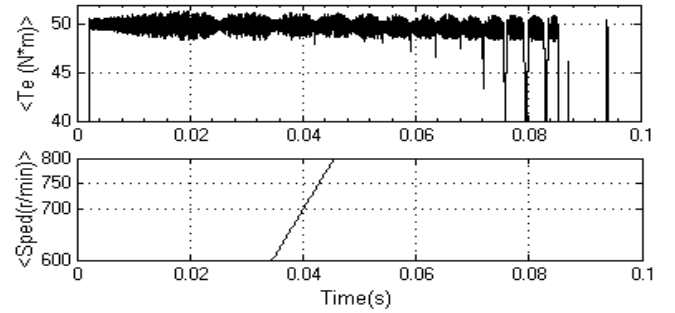


Fig. 7. The partial magnification of simulation results ( $\varphi=0.4\text{Wb}$ ).

##### C. Variable flux controller

###### 1) The structure of variable-flux controller

The variable-flux controller includes the PI speed regulator and linear fitting controller, as shown in Fig.6. The whole operation of the motor will be segmented two parts to control. That is to say the PI regulator is used to achieve the control of the flux amplitude before the speed of motor reaches the critical flux supersaturated speed; when the speed of motor is higher than the critical flux supersaturated speed, the linear fitting controller is used to adjust the amplitude of the given flux. And the determination of PI speed regulator has been introduced in chapter IV.A. So, we discuss the determination of linear fitting controller emphatically.

###### 2) Determination of linear fitting controller

For the speed testing point above the critical flux supersaturated speed, selecting the optimal amplitude of the flux during the operation of SRM at this speed.

Testing method: the given torque is 100N·m, the load torque is 50N·m, the given speed is 750r/min, changing the amplitude of the given flux (from 0.3 to 0.5). When the motor reaches the given speed, selecting the optimal amplitude of the given flux through the effect of torque ripple reduction. According to the simulation results, compared the torque ripple reduction effect in different amplitude of the given flux under the operating condition, thereby we can find that the optimal given flux is 0.395Wb when the speed of the motor reaches 750r/min. The

simulation results are shown in Fig.8.

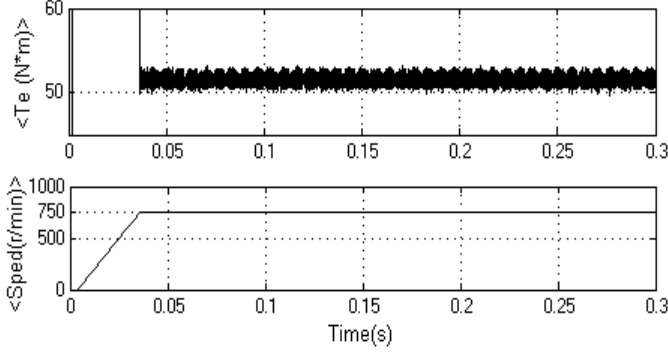


Fig. 8. The simulation result ( $\psi = 0.395\text{Wb}$ ).

Similarly, with 10r/min as a sampling step, using the above method to measure the optimal amplitude of the given flux from 750r/min to 1500r/min(the given speed is 1500r/min in simulation and experiment). And the linear fitting tool is used to linearly fit the speed-flux data obtained from the test. In order to ensure the enough output torque, if the flux is too small, it will be less saturated, which results the high torque ripple. Therefore, the given flux keeps constant when the speed higher than 1500r/min. Finally, we can conclude the equation of the variable flux model is:

$$\psi = \begin{cases} \text{the output of PI controller} & 0 \leq n < n_L \\ -0.0000955n + 0.472 & n_L \leq n < 1500 \\ 0.328 & n \geq 1500 \end{cases} \quad (10)$$

Where  $\psi$  — The given stator flux;

$n$  — The speed of the motor;

$n_L$  — The critical flux supersaturated speed.

## V. THE SYSTEM SIMULATION AND ANALYSIS

In this paper, the simulation results of traditional DTC system is used to compare with the results of three closed-loop DTC system with the variable-flux controller in Matlab/simulink. The parameters of the SRM(12/8) model are as follows: the given speed:  $W_r = 1500\text{r/min}$ , the given torque:  $T_e = 50\text{N}\cdot\text{m}$ , the initial torque of the load torque:  $T_L = 10\text{N}\cdot\text{m}$ , the initial stator resistance:  $R_s = 0.01\Omega$ , the inertia:  $J = 0.05\text{kg}\cdot\text{m}^2$ , the friction:  $F = 0.02\text{N}\cdot\text{m}\cdot\text{s}$ , the asymmetrical inductance:  $L_s = 0.67\text{Mh}$ , the symmetrical inductance:  $L_r = 23.6\text{Mh}$ , the saturated symmetrical inductance:  $L_m = 0.15\text{Mh}$ .

### A. The influence of variable-flux controller on efficiency

In order to verify the efficiency of the three closed-loop DTC system with variable flux for SRM, this paper compares the current waveform in traditional DTC system with the current waveform in three closed-loop DTC system with variable flux linkage. The simulated current waveform is shown in Fig.9 (a) and (b).

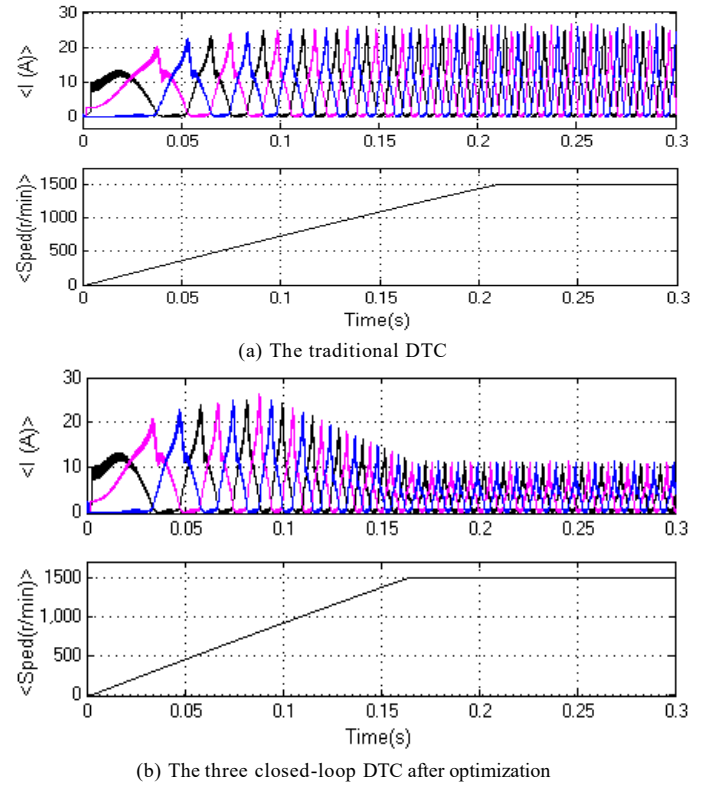
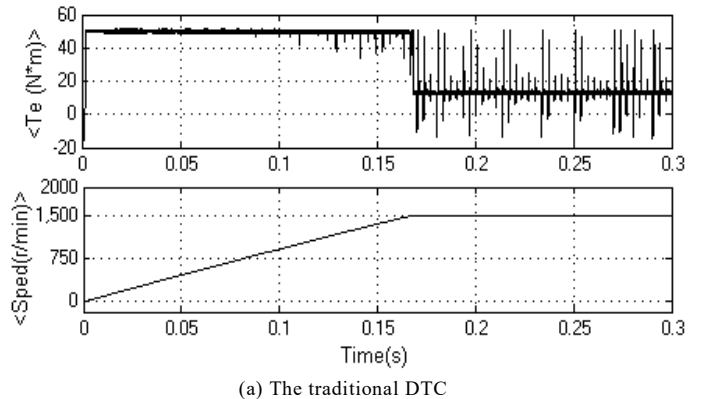


Fig. 9. The speed-current waveform.

Compared the current waveform before optimization with the current waveform after optimization, when the motor reaches the critical flux supersaturated speed, the magnetic flux amplitude is adjusted by the variable-flux controller. During the operation of SRM, the phase winding current obtained by the variable-flux optimization is smaller than the phase winding current under the traditional DTC system, thus greatly improving the running efficiency of SRM.

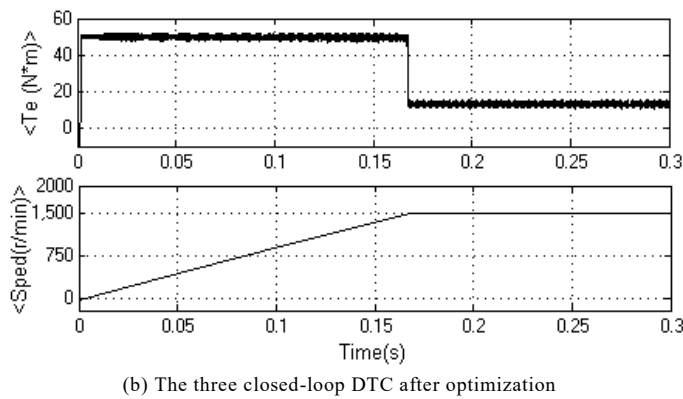
### B. The influence of variable-flux controller on torque ripple reduction

From the analysis for shortcomings of traditional DTC system in the chapter III.C, it can be seen that the torque ripple becomes higher with the increase of speed due to supersaturation of the flux, so the correctness of the variable-flux controller is verified. The simulation results are shown in Fig.10 (a) and (b).



(a) The traditional DTC





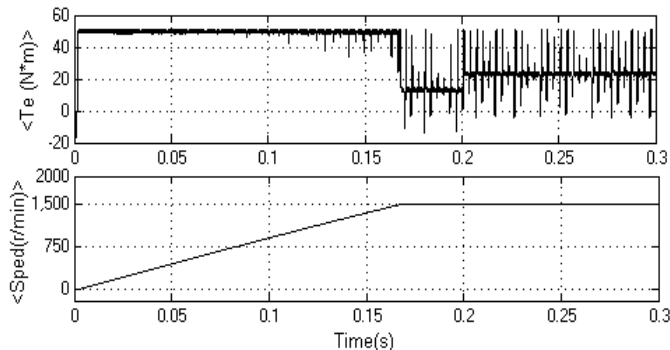
(b) The three closed-loop DTC after optimization

Fig. 10. The speed-torque waveform .

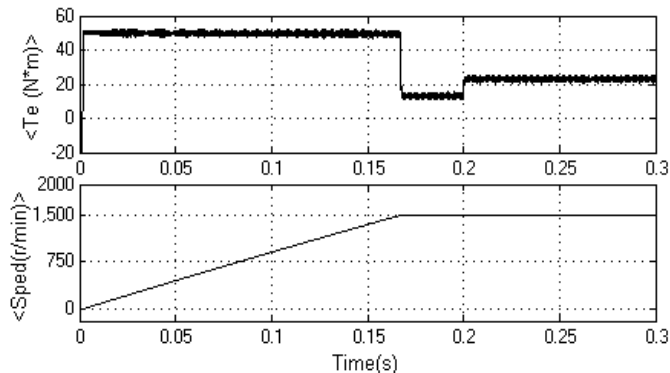
From the Fig.10 (a) and (b), it can be seen that the effect of the torque ripple reduction in three closed-loop DTC system optimized by the variable-flux is more obvious than the traditional DTC system, whatever the motor is in the started or steady state. According to Fig.10 (b), the torque ripple coefficient is about 8% ~ 10%.

C. The influence of variable-flux controller on stability

For any speed control system, a good stability is a basic requirement. So the three closed-loop DTC system with variable-flux controller is compared with the traditional DTC system, not only in the aspects of the efficiency and torque ripple reduction, but also in stability in this paper. The specific method is that the load is changed to 20N·m at 0.2s when the motor is running at steady state both in traditional DTC system and three closed-loop DTC system after optimization. The simulation results are shown in Fig.11 (a) and (b).



(a) The traditional DTC



(b) The three closed-loop DTC after optimization

Fig. 11. The speed-torque waveform.

It can be inferred from the simulation results in Fig.11 (a) and (b) that the torque ripple in the traditional DTC system is still large when the load is abruptly changed, whereas the torque ripple of the optimized DTC system is smaller and still within the allowable range. It can be concluded that the DTC system under variable-flux control strategy has good stability and anti-interference ability.

VI. EXPERIMENTAL PLATFORM AND RESULTS

In order to verify the effectiveness of variable-flux control algorithm, this paper takes a three-phase 12/8 pole SRM as the control target. And hardware experimental platform is shown in Fig.12. The parameters of the SRM are consistent with those in the simulation model. The parameters of the key elements are listed in the TABLE. I.

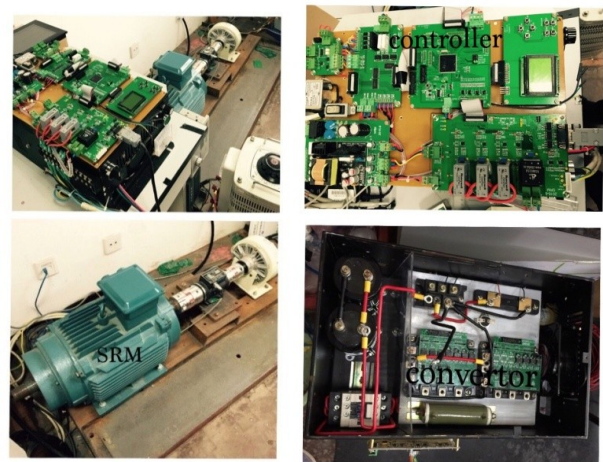


Fig. 12. SRM hardware test platform.

TABLE I  
THE PARAMETERS OF THE KEY ELEMENTS

Key Elements	Key Parameters	Value
SRM	Number of stator/rotor	12/8
	Number of phase	3
	Given voltage(V)	150
	Given speed(r/min)	1500
	Load torque(N·m)	5
Intelligent power module (PM50RSA120)	Power(Kw)	15
	Maximum of frequency(KHz)	20
TMS320F2812	Operating frequency(KHz)	15
	Main frequency(MHz)	120
Magnetic powder brake (TJ-POD-5)	Maximum of braking torque (N·m)	50
Oscilloscope (DSOX4024A)	Maximum sampling frequency (MHz)	4

*A. Experiments on efficiency*

Fig.13(a) is the three-phase current waveform in traditional DTC system, when the motor reaches the given speed, the peak-peak value of the current is 15.4A, the average of the current is 4.495A.

Fig.13(b) is the three-phase current waveform in the three closed-loop DTC speed control system optimized by variable-flux controller. The peak-peak value of the current is 12.4A and the average of the current is 3.418A.

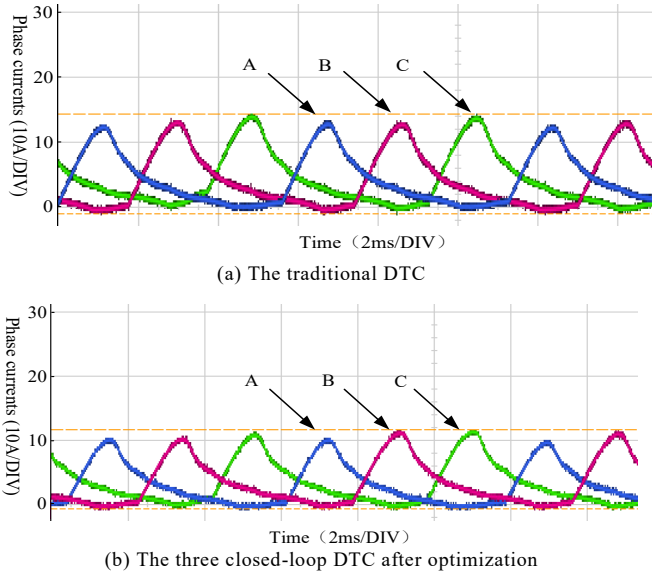


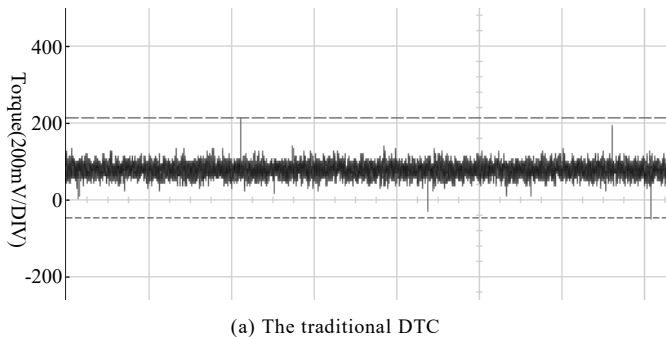
Fig. 13. The waveform of the three-phase currents.

From the Fig.13 (a) and (b) , it can be seen that the three-phase current is basically symmetrical at the same circumstances, both (a) and (b). But the peak-peak or average value of the current in the optimized DTC system are smaller, which greatly reduces the copper consumption of the stator phase winding and improves the operating efficiency of the system.

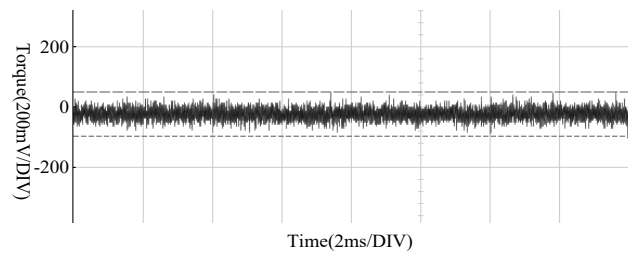
*B. Experiments on torque ripple*

Fig.14(a) is the torque waveform in traditional DTC system. When the motor reaches the given speed, the peak-to-peak value of torque ripple is 261mV.

Fig.14(b) is the torque waveform in the three- closed-loop DTC system optimized by the variable-flux controller. When the motor reaches the given speed, the peak-to-peak value of torque ripple is 147mV.



(a) The traditional DTC



(b) The three closed-loop DTC after optimization

Fig. 14. The waveform of the three-phase currents.

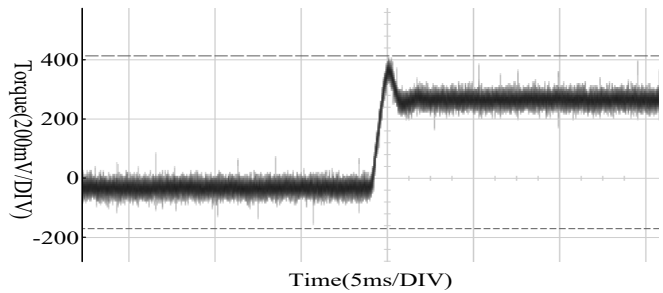
Compared with Fig.14 (a) and (b), it can be seen that the torque reduction effect of three closed-loop DTC system after optimization is obvious and the noise suppression effect is remarkable.

*C. Experiments on the stability*

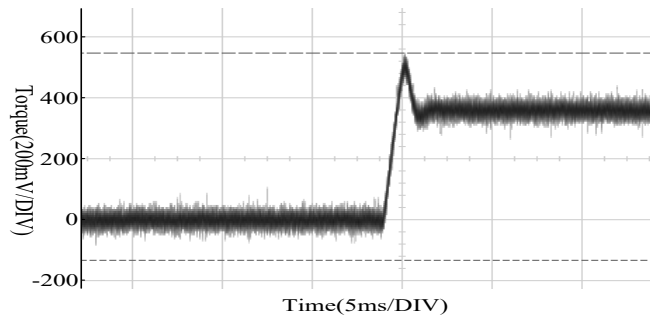
In order to verify the stability of DTC system after optimization, the traditional DTC speed control system and the three closed-loop DTC speed control system optimized by the variable-flux controller are tested for torque mutation.

Fig.15 (a) is the torque mutation waveform for the traditional DTC speed control system when the load torque is from 5N·m to 11N·m.

Fig.15(b) is the torque mutation waveform for the three closed-loop DTC speed control system optimized by variable-flux controller when the load torque is from 5N·m to 12N·m.



(a) The traditional DTC



(b) The three closed-loop DTC after optimization

Fig. 15. The torque mutation waveform.

Compared the Fig.15 (a) with (b), it can be seen that the three closed-loop DTC system optimized by the variable-flux controller has better system stability, no matter before or after the transition.

Note: In the process of the experiment, the magnetic powder brake(TJ-POD-5) is used as the load of the motor, so the size of

the motor's load can not be given accurately. Although the value of torque mutation in three closed-loop DTC system is larger than that in the traditional DTC system, the final experimental result of DTC system after optimization is still superior to the traditional DTC system. This shows that the three closed-loop DTC system after optimization has better system stability.

## VII. CONCLUSION

In this paper, through the detailed analysis on the problems existed in the traditional DTC system for SRM, the control theory of variable flux is applied into it, and the concept of critical flux supersaturated speed is put forward. Then, a three closed-loop DTC system with variable flux is built, realizing the double closed-loop tracking for the torque and flux, solving the problems of the low operation efficiency, higher torque ripple and the poor system stability in traditional DTC speed control system. Finally, through the simulated and experimental comparison, we can see that the performance of the three closed-loop DTC system optimized by the variable-flux strategy has been greatly improved, which provides a solid theoretical basis for the extensive application of SRM.

## REFERENCES

- [1] X. L. Wang, Z. L. Xu, "Speed regulation control of switched reluctance motors based on PI parameter self-adaptation", *Proceedings of the CSEE*, vol. 35, no. 16, pp. 4215-4223, 2015.
- [2] J. B. Sun, Q. H. Zhan, S. H. Wang, Z. Y. Ma., "Control strategy of switched reluctance motor to restrain vibration acoustic noise and torque ripple", *Proceedings of the CSEE*, vol. 28, no. 20, pp. 134-138, 2008.
- [3] J. Pan, N. C. Cheng, J. Yang., "High-precision position control of a novel planar switched reluctance motor", *IEEE Trans. Ind. Electron*, vol. 52, no. 6, pp. 1644-1652, 2005.
- [4] X. D. X, K. W. E. Cheng, S. L. Ho. , "A self-training numerical method to calculate the magnetic characteristics for switched reluctance motor drive", *IEEE Trans. Magn*, vol. 40, no. 2, pp. 734-737, 2004.
- [5] S. Paramasivam, S. Vijayan, M. Vasudevan, R. Arumugam, R. Krishnan. , "Real-time verification of AI based rotor position estimation techniques for a 6/4 pole switched reluctance motor drive". *IEEE. Trans. Magn*, vol. 43, no. 7, pp. 3209-3212, 2007
- [6] C. Choi, D. Lee, K. Park., "Fuzzy design of a switched reluctance motor based on the torque profile optimization". *IEEE Trans. Magn*, vol. 36, no. 5, pp. 3548-3550, 2000.
- [7] W. F. Shang, S. D. Zhao, etc., "A sliding mode flux-linkage controller with integral compensation for switched reluctance motor". *IEEE Transactions on Magnetics*, vol. 45, no. 9, pp. 3322-3328, 2009.
- [8] S. K. Sahoo, S. K. Panda, J. X. Xu, "Indirect torque control of switched reluctance motors using iterative learning control", *IEEE Transactions on Power Electronics*, vol. 20, no. 1, pp. 200-208, 2005.
- [9] C. K. Kim, I. J. Ha. (1996). "A new approach to feedback-linearizing control of variable reluctance motors for direct-drive applications", *IEEE Transactions on Control System Technology*, vol. 4, no. 4, pp. 348-362, 1996.
- [10] H. T. Zheng, J. P. Jiang. "Study on high-grade torque control strategy for switched reluctance motor". *Transactions of China Electrotechnical Society*, vol. 20, no. 9, pp. 24-28, 2005.
- [11] P. V. Vladan.(2012). "Minimization of torque ripple and copper losses in switched reluctance drive", *IEEE Transactions Power Electronics*, vol.27, no. 1, pp. 388-399, 2012.
- [12] H. F. Nisai, M. Marcus, B. I. Robert. "High-dynamic four-quadrant switched reluctance drive based on DITC". *IEEE Transactions on Industry Applications*, vol. 41, no. 5, pp. 1232-1242, 2005.
- [13] A. D. Xu, Y. H. Fan, Z. Q. Li. "SRM torque ripple minimization based on space voltage vector". *Electric machines and control*, vol. 14, no. 1, pp. 35-46, 2010.
- [14] C. L. Xia, Z. R. Chen, B. Li. "Instantaneous torque control of switched reluctance based on RBF neural network". *Proceedings of the CSEE*, vol. 26, no. 19, pp. 127-132, 2006.
- [15] J. F. Xiao, Y. B. Hou, R. Wang, etc. "The research on the variable flux DTC for switched reluctance motor based on BP neural network". *Electronic Technology*, vol. 01, no. 08, pp. 16-27, 2015.
- [16] M. H. Wang. "Research of DTC Speed adjusting system structure for SRM". *Electronic Drive*, vol. 42, no. 08, pp. 3-5+46, 2012.
- [17] Z. H. Hu, Y. Li, K. K. Wang. "Torque ripple reduction of SRM based on direct torque control". *Machine & Electrical Apparatus*, vol. 35, no. 3, pp. 34-39, 2016.
- [18] A. D. Cheok, Y. Fukuda. "A new torque and flux control method for switched reluctance motor drives". *IEEE Transactions on Power Electronics*, vol. 20, no.9, pp. 543-557, 2002.
- [19] H. X. Wu, Theory and control technology of switched reluctance motor system. Beijing: *China Electric Power Press*, 2010, pp. 25-26.
- [20] H, J, Guo. "Considerations of Direct Torque Control for Switched Reluctance Motors". *IEEE ISIE*, vol. 5, no. 6,, pp. 2321-2325,2006.



and motor drives.

**Xianchao Zhao** was born in Qingdao, Shandong province, China in 1991. He received the B.S. degrees in electrical engineering and automation from the Linyi University in 2015, was a master degree candidate in Dalian Maritime University and majored in electric science and technology. His research interests include motion control



and motor drives.

**Aide Xu** was born in Rizhao, Shandong province, China in 1974. She received the Ph.D. degree in marine engineering from the Dalian Maritime University in 2010. Currently, she is a professor with the Department of Electrical Engineering, faculty of College of Information Science and Technology, Dalian Maritime University. Her research interests include



and motor drives.

**Wen Zhang** was born in Harbin, Heilongjiang province, China in 1992. She received the B.S. degrees in electrical engineering and automation from the Yunnan Nationalities University in 2015. was a master degree candidate in Dalian Maritime University and majored in electric science and technology. Her research interests include motion control